

Composite Materials Using Mallow Fibers and Epoxy Resin

Materiais Compósitos usando Fibra de Malva e Resina Epóxi

Wamber Broni de Souza,^{a,*} Genilson Pereira Santana,^a Dorian Lesca de Oliveira,^a Antônio Claudio Kieling,^b Gilberto Garcia del Pino,^b Sérgio Duvoisin Júnior,^c José Costa de Macêdo Neto^d

^aUniversidade Federal do Amazonas, Instituto de Ciências Exatas, Departamento de Química, Programa de Pós-Graduação em Química, CEP 69067-000, Manaus-AM, Brasil

^bUniversidade do Estado do Amazonas, Escola Superior de Tecnologia, Departamento de Engenharia Mecânica, CEP 69065-001, Manaus-AM, Brasil

^cUniversidade do Estado do Amazonas, Escola Superior de Tecnologia, CEP 69065-001, Manaus-AM, Brasil

^dUniversidade do Estado do Amazonas, Escola Superior de Tecnologia, Departamento de Engenharia de Materiais, CEP 69065-001, Manaus-AM, Brasil

*E-mail: wambersa@ufam.edu.br

Recebido: 11 de Julho de 2023

Aceito: 15 de Dezembro de 2023

Publicado online: 9 de Janeiro de 2024

This work investigates chemically modified Mallow fibers (MF) and their utilization as reinforcement in an epoxy composite. The untreated Mallow fibers (UTMF) and the Mallow fibers treated (TMF) with 5% NaOH solution were characterized, and Mallow/epoxy resin composites (MEC) were fabricated using 10, 20, and 30 wt.% of TMF, and their mechanical, and thermal properties were studied. UTMF, TMF, and MEC were evaluated using Fourier-transform Infrared Spectroscopy (FTIR), Differential Scanning Calorimetry (DSC)-Thermogravimetric Analysis (TGA), X-ray diffraction (XRD), and scanning electron microscopy (SEM). A tensile test was performed to characterize the MEC. The alkali treatment increased cellulose by 7% and lignin by 56%, removed hemicellulose and ash content up to 28.8% and 31.4% respectively, and reduced moisture by 3.5%. The spectra of the FTIR and DSC-TGA analyses show the broad absorption and decomposition characteristics of cellulose, hemicellulose, and lignin in the fibers. The UTMF presented a crystallinity index (C_1) value of 57% while the TMF had a C_1 value of 77.60%. From the results, it is observed that the maximum tensile strength value was obtained at 20 wt.% of fiber loading, giving 100.22 MPa, which is considered ideal for the fabrication of Mallow/epoxy resin composites.

Keywords: Mallow fiber; alkali treatment; mechanical properties; composite materials; epoxy resin.

1. Introduction

The most common synthetic fibers^{1,2} used in the composites industry are glass fibers,³⁻⁶ carbon fibers,⁷⁻¹⁰ and Kevlar® (aramid).¹¹ However, the production of these fibers uses non-renewable natural resources, materials that are not eco-friendly, that have a high cost of production, and consume large amounts of water and energy in their production, in addition to generating industrial waste. To preserve the environment, there is a great interest in discovering environmentally compatible materials that can replace or reduce the use of synthetic fibers, among these, natural fibers stand out.

Plant fibers are widely recognized by the industry and are the most extensively studied by researchers because they are light, biodegradable, and resistant.¹² Investigations have been carried out on numerous natural fibers, such as Mallow, jute, sisal, curauá (*Ananas erectifolius*), banana, cotton, bamboo, bagasse, flax, kenaf (*Hibiscus cannabinus*), oats, barley, wheat, rice husk, wood, alginate, and hemp, for the manufacture of natural fiber polymer composites. The growth in research involving natural fibers can be explained by a short growth period, renewability, lower production costs, good specific mechanical properties, lower density of the composites, reduced energy consumption during manufacturing, biodegradability and eco-friendly materials, lower risk to human health, and broader viability of the product.¹² Cellulose, hemicellulose, and lignin constitute the vegetable fibers that can be obtained from the stem, bast, leaves, seeds, fruit, wood, stalk, and grass/reeds.¹³

Among the natural fibers, Mallow fiber presents relatively very few reports in the literature, and its uses for industrial applications like the automotive¹⁴ and construction industries are even rare.¹⁵ Mallow belongs to the *Malvaceae* family, which comprises several species such as *Malva sylvestris* and the *Urena lobata* Linn. It is originally from Asia and is today cultivated in meadows of rivers, particularly in the Amazon region of Brazil.

In Brazil, Mallow has been cultivated in the states of Amazonas and Pará since the 1930s. It is a plant that is well adapted to soils of low fertility and can be cultivated in *terra firme* soil. The production of Mallow and jute fibers was for a long time the activity that was responsible for a significant percentage of the formation of income in the state of Amazonas (20% of the income

in the primary sector), and many families of the region were employed in this sector, mainly as family labor.¹⁶

In recent decades, there has been a decrease in the extraction of these fibers that are used in the production of sacks, carpets, paper, upholstery, clothing, etc., due to several factors such as the low price paid per ton of the product, and the replacement of the natural fiber by synthetic fibers, etc. With recent studies using Mallow fibers as reinforcements in composites, preliminary results have indicated excellent properties to be explored, and these plantations have the potential to become a reference activity once again for the economy in the Brazilian Amazon,¹⁷ since jute and Mallow are linked to sustainable development in rural areas via family farming.

An increase in the production of jute and Mallow chain could be an alternative for increasing the income of the population in the interior of the state of Amazonas. The state of Amazonas presents areas with floodplains that are appropriate for the production of jute and Mallow, in addition to having the riverine populations for planting and harvesting.¹⁸

Researchers have already carried out studies utilizing Mallow fibers as the reinforcement in either thermoplastic or thermosetting polymers and obtained good results concerning the mechanical and thermal properties. One study investigated the mechanical properties of epoxy composites with high incorporation of Mallow fibers and found that composites with 20%¹⁹ and 30%^{20,21} of fibers in the volume provide the highest tensile strength.

Several applications using composite materials reinforced with natural fibers have been reported in the literature²²⁻²⁵ in several industries, such as the aerospace industry, in the construction of wings and control surfaces;²⁶ the automotive industry, in car parts such as door panels, seat backs, dashboards, boot-liners, and instrument panels, etc.;²⁷ and in the defense industry, in helmets and bulletproof jackets.^{28,29-31}

Thus, this study aims to characterize Mallow fibers and their utilization as a reinforcement in a polymer matrix. For this purpose, the fibers were first characterized, and then composites were fabricated using 10, 20, and 30 wt.% of treated fibers, and their mechanical, and thermal properties were studied to establish their suitability in various engineering applications.

2. Experimental

2.1. Mallow fiber and epoxy resin

The Mallow fibers investigated in this work were of the species *Urena lobata* Linn., commercially supplied by the Brazilian firm Castanhal Textil (Manacapuru, AM). Figures 1a and 1b illustrate the bundles of Mallow fibers received, as well as some long, continuous fibers separated for reinforcing the composite. As the composite matrix, the epoxy resin and hardener in a stoichiometric proportion of 2:1 (resin/hardener) were supplied by Redelease Ltd (São Paulo, Brazil).

2.2. Chemical treatment

After delivery, the fibers were cleaned and combed to untangle them and remove impurities, then cut to a length of 16 cm (Figure 2a). Subsequently, the fibers were subjected to chemical treatment with 5% sodium hydroxide in the solution. Figure 2b shows the immersion of the fibers in the solutions for a period of 4 hours. Treatment with 5% NaOH and immersion time of 4 hours promotes an increase in crystallinity in Mallow fibers and, consequently, in surface roughness, in addition to the direct relationship with mechanical strength and modulus of elasticity.^{32,33} Excess alkalinity and/or exposure time can damage the fiber as it removes a portion of the crystalline structure, thereby reducing its mechanical performance.³⁴⁻³⁶ After removing the fibers from the solution, they were washed several times with distilled water until a neutral pH was obtained and then dried at room temperature in a closed room for 7 days. Before using the fibers in the composites, the samples were dried in an oven for 60 minutes at 100 °C to eliminate moisture.

2.3. Cellulose and lignin composition analysis of UTMF and TMF

The Van Soest methodology³⁷ was utilized to analyze the chemical components of the vegetable fibers. This comprehensive approach involved employing a variety of

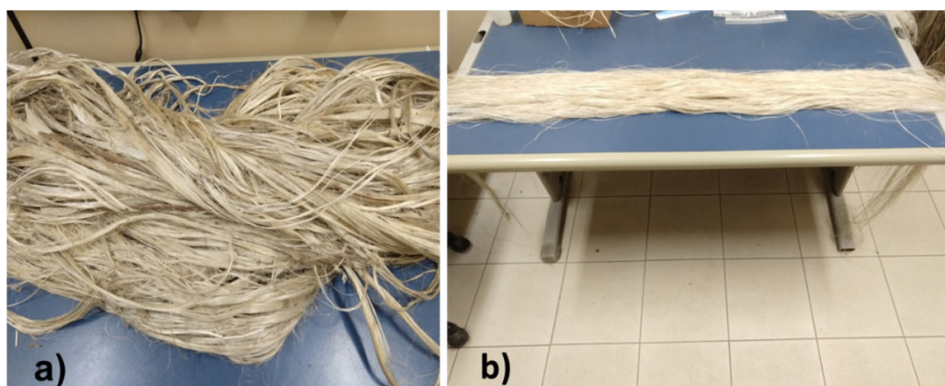


Figure 1. (a) Bundle of Mallow fiber (b) long continuous fibers

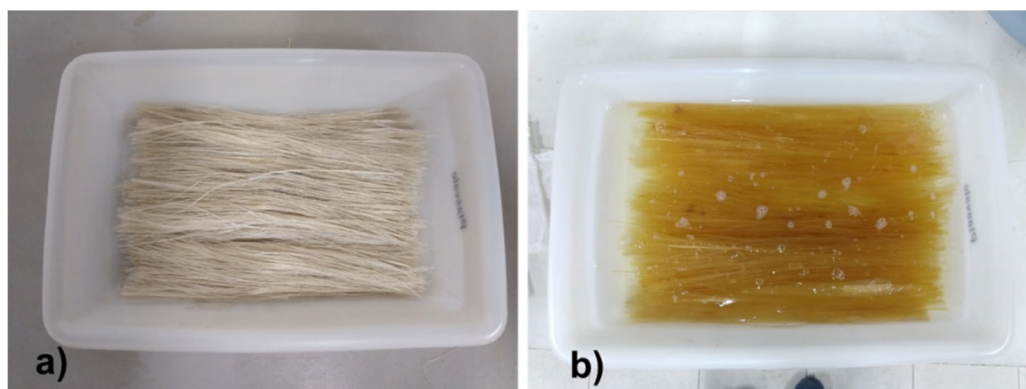


Figure 2. (a) Fibers cut to 16 cm (b) and during chemical treatment

solutions, including neutral detergent solution (comprised of EDTA, hydrated sodium borate, anhydrous sodium phosphate, sodium lauryl sulfate, ethylene glycol, and amylase), acid detergent solution (featuring cetyl trimethyl ammonium bromide and H_2SO_4), and 72% sulfuric acid solution. These solutions were skillfully utilized to differentiate the diverse fractions of hemicellulose, cellulose, and lignin, as depicted in Figure 3.

2.4. Determination of moisture content

Initially, the sample was pre-dried in an oven with forced air circulation at 55 to 60 °C for 48 to 72 hours. Then it was ground, homogenized, and dried again in an oven at 105 °C

for 4 to 16 hours. The percentage of moisture was calculated using the following equation: % moisture = 100% - final content of dry matter.

2.5. Preparation of the Mallow-epoxy composite

Figure 4 shows the composites with 10% (Figure 4c), 20% (Figure 4d), and 30% (Figure 4e) of aligned Mallow fibers, which were manufactured in a mold with a female cavity in a plate and another male plate that penetrates the cavity to be able to apply pressure on the composite material. The cavity plate has 15 mm parallel grooves for fixing the fibers and for the removal of excess resin (Figure 4a). The thickness is calculated as the volume divided by the area:

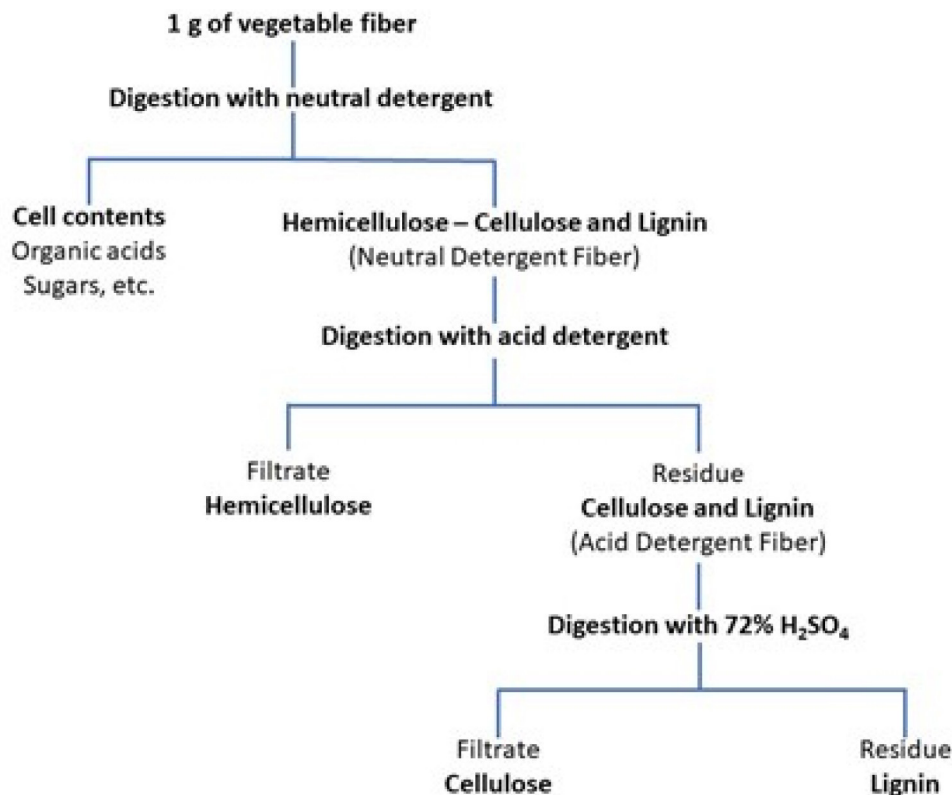


Figure 3. Determination of Cellulose, and Lignin Composition Analysis of UTMF and TMF by Van Soest methodology³⁷

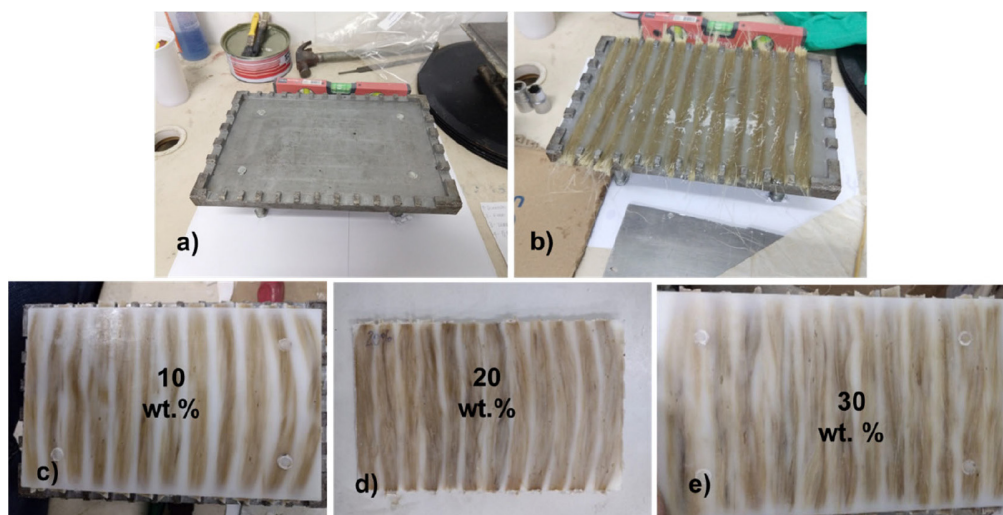


Figure 4. Composites with 10 wt.%, 20 wt.%, and 30 wt.% in volume of aligned Mallow fibers

$(15 \text{ mm} \times 15 \text{ mm} \times 3 \text{ mm}) / (15 \text{ mm} \times 15 \text{ mm}) = 3 \text{ mm}$. The corresponding amount of resin and hardener was placed in a beaker and stirred for 15 minutes. Then, a layer of resin was placed in the cavity, and, after, the fibers were placed in the cavity (Figure 4b). After all the fibers were in place, the rest of the corresponding resin was introduced into the mold, which was then left to stand for 5 minutes. Following this, the lid (male) was put on and pressure was applied (10 MPa).

The mold was maintained under pressure at room temperature (RT) for 24 hours during the curing of the resin. When cured, the rectangular plates were cut into 12 samples, maintaining the fiber aligned along the length (Figure 5)

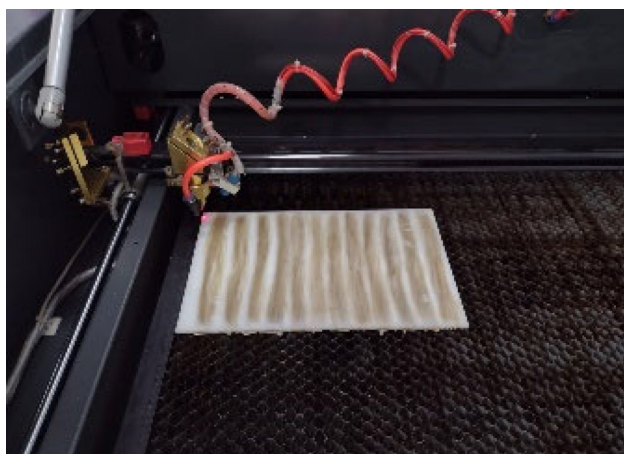


Figure 5. Image shows the cured rectangular plates being cut

2.6. Differential scanning calorimetry and thermogravimetry analysis

For the differential scanning calorimetry (DSC) analyses and measurement of mass loss (TGA), the UTMF and TMF samples were comminuted and placed in aluminum crucibles using a simultaneous thermal analyzer (SDT Q600 V20.9 BUILD 20, TA INSTRUMENTS) with a measurement range from 0 to 1500 °C, nitrogen flow of

30 mL min⁻¹, ramp rate of 10 °C min⁻¹, considering the recommendations of ASTM D3418-03.³⁸

2.7. Microstructural analysis

The morphological analysis of the surface of the UTMF and TMF samples and the microstructural analysis were performed on fractured surfaces of MEC (10, 20, and 30%) tensile samples using a scanning electron microscope (JSM-ITR 500 HR, Jeol) with an accelerating voltage of 0.3 to 30 kV. The samples were metalized with gold for five minutes using a high vacuum metallizer (DII-29010SCTR Smart Coater, Jeol, Japan).³⁹

2.8. Tensile tests

Tensile tests were performed to determine the mechanical strength of each composite of the MEC according to ASTM D638.⁴⁰ A universal testing machine (Instron 5984) equipped with a 150 kN load cell was used to perform traction tests at 3 mm min⁻¹ at room temperature (23 ± 2 °C, RH 50 ± 10%).

2.9. Characterization of UTMF and TMF

To ascertain the structural and compositional constitution of the UTMF, and the changes that occurred after the alkaline treatment, X-ray diffraction (XRD) analysis was carried out. This was done using a diffractometer (XRD-7000, Shimadzu) operating under CuK α radiation at a voltage of 40 kV and 30 mA, with a scanning rate of 2 °C min⁻¹.

The XRD was also used to calculate the crystallinity index values of UTMF and TMF. The crystallinity index (C_c) for cellulose was calculated using equation 1, where I_1 is the intensity of the diffraction minimum, which is related to the amorphous part, and I_2 is the intensity of the diffraction maximum, which is related to the crystalline part. This method was developed by Segal and collaborators (1959) and has been widely used for the study of natural fibers.^{41,42}

$$C_I = 1 - \frac{I_1}{I_2} \quad (1)$$

3. Results and Discussion

3.1. Chemical composition analysis of Mallow fibers

The results of the chemical composition analysis before and after treatment of the Mallow fibers with 5% NaOH are presented in Table 1.

Table 1. Chemical composition of Mallow fibers before and after alkali treatment

Chemical Composition	Mallow Fibers (%)	
	Untreated	Treated
Cellulose	75.39	80.59
Hemicellulose	17.40	12.39
Lignin	2.47	3.87
Ash	0.70	0.48
Moisture	7.30	7.04

This alkali treatment is important because removing the hemicelluloses, lignin, waxes, and other compounds occurring in lesser amounts in the fiber results in roughening of the fibers and can enhance the mechanical interlocking between the fibers and the polymer during the production of the composite.⁴³ In this work, the treatment removed hemicellulose and the ash content by up to 28.8 and 31.4%, respectively, but at the same time, the lignin increased by 56%. This may be because the structure of fibers is strongly related to the age of the plant, its species, climate, harvesting time, fiber processing techniques,⁴⁴ and non-uniform compositions.⁴⁵ The cellulose part increased by 7% after the treatment and it is the key component that gives the fiber strength, rigidity, and stability.⁴⁶ Hemicelluloses are closely linked to cellulose microfibrils and help embed the cellulose in a matrix⁴⁷ and lignin functions as a chemical adhesive within and

between fibers.⁴⁸ The moisture was reduced by 3.5% after the treatment.

3.2. Mallow fiber morphology

Fiber morphology is important in order to be able to predict the interaction of the fibers with the polymer matrix in natural fiber-reinforced composites. Figure 6 shows the micrographs of the UTMF (a) and TMF (b) at magnification levels of 220×, respectively. The fibrils of UTMF (Figure 6a) appear to be joined, forming a single bundle of fibers,^{49,50} and show a smooth, compact surface with no fibrillation. In contrast, the TMF (Figure 6b) reveals an increase in surface roughness, mainly due to the chemical degradation of the hemicellulose as a result of the alkali treatment.⁴⁹⁻⁵¹ This modification of the fiber surface can improve its physical adhesion with the matrix phase, since it can facilitate the penetration into the internal parts of the fiber, increasing, consequently, the mechanical properties of the composite material.⁵² In addition, the microfibrillar angle can also be modified by the removal of the hemicellulose, which directly affects the increase in fiber stiffness.³⁴⁻³⁶

3.3. Characterization of UTMF and TMF

The results of the FTIR spectroscopy for the UTMF, TMF, and MEC are shown in Figure 7. The figure shows the variation in peaks in the range of 4000 – 400 cm⁻¹. The spectra obtained for both the UTMF, TMF, and MEC show broad O–H absorption elongation at 3367, 3348, and 3352 cm⁻¹, respectively, which is characteristic of cellulose, hemicellulose, and lignin in the fibers.^{53,54} The alkane C–H absorption elongation of cellulose, hemicellulose, and lignin (2860–2970 cm⁻¹), which is characteristic of natural fibers, is found in both UTMF, TMF, and MEC. A peak is observed in UTMF at band 1735 cm⁻¹ that is not present in TMF and MEC. This peak may be due to the removal of unwanted materials like wax from the surface of the fiber after the chemical treatment¹⁹ and may be related to C=O stretching of acetyl or carboxylic ester. The absorption band at 1238 cm⁻¹ corresponds to C=O and –C–O–C groups of

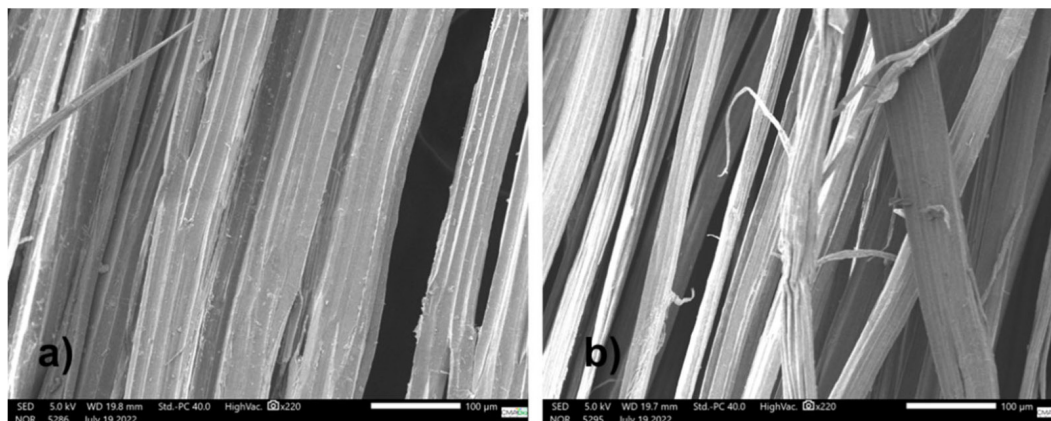


Figure 6. (a) SEM micrographs of UTMF (b) TMF micrographs of UTMF

lignin. The absorption band at 1033 cm^{-1} corresponds to the C–O elongation of cellulose, hemicellulose, and lignin. Therefore, absorption bands at 891 to 559 cm^{-1} are taken to be C=C bending of lignin.

In the literature, there are several discussions about the spectrum of the FTIR of pure epoxy.^{55,56} The broad band at 3437 cm^{-1} is attributed to the symmetrical stretching vibration of the –OH which has been shifted to 3352 cm^{-1} in Mallow fiber composite (MEC). As a rule of thumb, the –OH stretching peak is sensitive to hydrogen bonding. The band at 2924 – 2866 cm^{-1} is more pronounced in Mallow fiber composite as compared with neat epoxy, UTMF, and TMF, which is due to C–H stretching at 1735 and 1675 cm^{-1} are found in the pure epoxy spectrum and the bands at 1735 cm^{-1} (UTMF) and 1593 cm^{-1} (TMF) are not found in the MEC. The band around 1608 cm^{-1} that appears in MEC is due to the C=C bond in the epoxy and appears in UTMF and TMF due to the presence of these bonds in lignin. Furthermore, a high difference was found in the MEC fingerprint region (1608 – 600 cm^{-1}) compared to UTMF and TMF. This may be due to the active participation of fibers as reinforcement in the matrix.

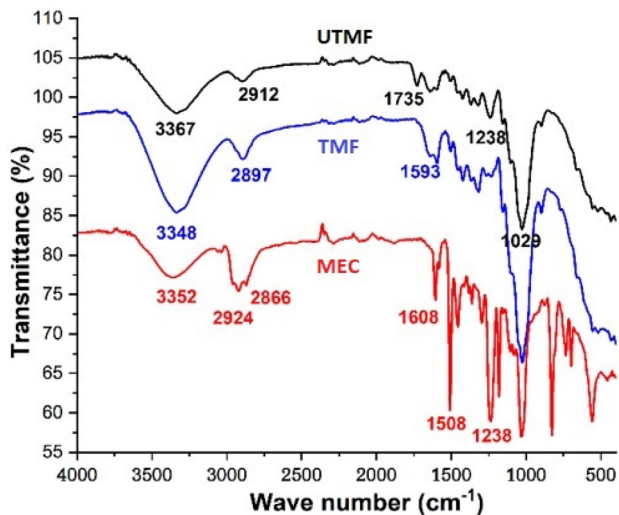


Figure 7. FTIR spectra of UTMF, TMF, and MEC samples

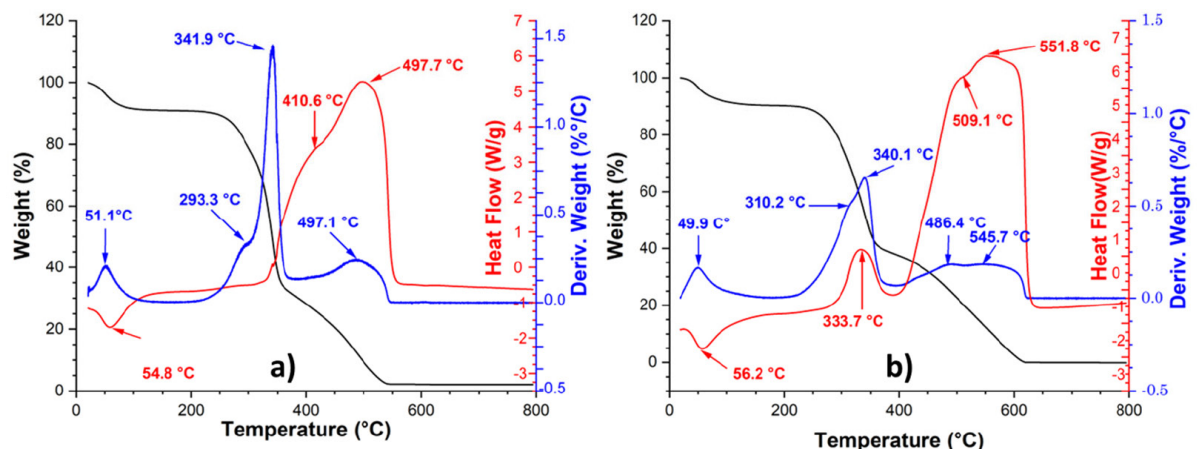


Figure 8. (a) DSC and TGA graph of UTMF samples (b) TGA graph of UTMF samples

Figure 8 shows the DSC-TGA curves of UTMF (a) and TMF (b). In the UTMF (Figure 8a), the peak of 51.1 °C represents the loss of surface water from the sample in the TGA/DTG and DSC analyses. The first transition peak, in the 293.3 °C curve, refers to the decomposition of hemicellulose.^{49,57} The decomposition of cellulose is indicated by the peak at 341.9 °C . The thermal decomposition of lignin begins only at higher temperatures (over 400 °C). Due to its complex structure, lignin is the most difficult component to degrade among the three main components.^{41,49}

In the DSC graph, it is possible to notice events of water loss and thermal decomposition of the hemicellulose, cellulose, and lignin that correspond to those found in the TGA/DTG curves. In the DSC curve, the endothermic peak around 54.8 °C is associated with loss of water through vaporization. Even though the fibers were previously dried before each analysis, the elimination of water is hampered by its hydrophilic character. In addition to the endothermic peak originating from the evaporation of water, the DSC curve of the untreated fiber shows two more thermal events (at 410.6 and 497.7 °C) that are of an exothermic nature, which are characteristic of the constituents of the fiber, *i.e.*, cellulose, hemicellulose, and lignin.

Thermal decomposition of hemicellulose and cellulose occurs at temperatures over 300 °C and up to approximately 410.6 °C . Finally, the last event (at 497.7 °C) refers to the decomposition of lignin.⁵⁸⁻⁶⁰

Figure 8b shows the DSC and TGA graph of TMF. The peak of 333.7 °C in the DSC curve, which is more evident in the TMF than in the UTMF, refers to the decomposition of cellulose. This greater evidence is probably due to the increase in Cellulose content after treatment with NaOH, in addition to different reactions or mechanisms involved in the process. In the TGA/DTG graph, it is possible to notice events of water loss (49.9 °C) and thermal decomposition of the hemicellulose (310.2 °C), cellulose (340.1 °C) and lignin (486.4 °C) that correspond to those found in the DSC curves. In the last point of decomposition (Figure 8b), at temperatures over 545.7 °C (TGA/DTG and DSC analyses)

which indicates the probable decomposition of sodium hydroxide.

The thermodegradation of polysaccharides as hemicellulose consists of various saccharides, amorphous structure, rich in branches, which are very easy to remove from the main stem, and the cellulose that consists of a long polymer of glucose without branches, its structure is in good order and very strong, can occur by cleavage of glycosidic, C–H, C–O, and C–C bonds, dehydration, decarboxylation, and decarbonylation reactions, with formation of C–C, C–C, C–O bonds as well as carbonyl and carboxyl groups.^{49,58,60} The weight loss of Lignin which features a structure full of aromatic rings with various branches, occurs at higher temperatures and its degradation is related to dehydration, yielding derivatives with lateral unsaturated chains, and the release of water, CO₂, CO, and methane.^{49,58} The differences in the inherent structures and chemical nature are responsible for the different behaviors observed.⁵⁸

The DSC and TGA analyses for both types of fibers (UTMF and TMF) showed only a slight displacement of the peaks, though within an acceptable range.

3.4. Crystallinity index of UTMF and TMF

The X-ray diffractograms, XRD, of Mallow fiber are shown in Figure 9. Three peaks were observed for all samples at $2\theta = 15.8$, 22.3 , and 34.5° . These are characteristic of the crystal polymorph I of cellulose. For fibers with higher cellulose content, like cotton or flax, two peaks around 16° are observed in curaua fibers, only one broad peak was observed^{49,50} and for Mallow fibers (UTMF and TMF) only one broad peak was observed due to the presence of amorphous materials like lignin, hemicelluloses, and amorphous cellulose, which cover the two peaks.^{56,61,62}

The crystallinity index (C_1) results for UTMF and TMF show the UTMF presented a C_1 of 57% while the TMF had a C_1 of 77.60%, indicating the effectiveness of the chemical treatment removed of some of the amorphous constituents of the fibers, likewise, it may have occurred

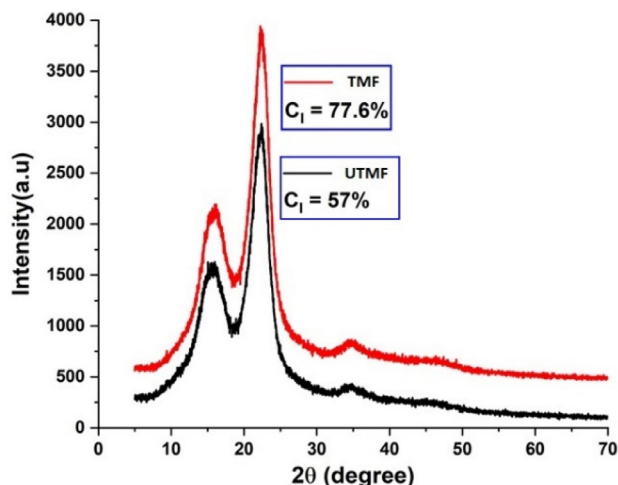


Figure 9. XRD patterns of TMF and UTMF samples.

to rearrangement of the crystalline regions in such a way that the fiber shows a more crystalline.⁶³ Crystallinity is related to the cellulose content that the fiber has, as it is the only component that crystallizes.⁶⁴ In the cellulosic chain, intramolecular hydrogen bonds are responsible for imparting the mechanical properties of stiffness and strength. According to several authors, the C_1 of natural fiber is directly related to the increase in mechanical strength and modulus of elasticity, although it is not the only factor that determines the increase or reduction of these properties.⁶⁵

3.5. Mechanical properties of the MEC

The mechanical properties, such as tensile strength, Young's modulus, and elongation at maximum load, of the fiber composites treated with alkali at different weight percentages (10, 20, and 30 wt.%) were measured and presented in Figure 10. From the results, it is observed that the maximum value for the mechanical properties was obtained at 20 wt.% of fiber loading, which gives 100.22 MPa of tensile strength, 4.59 GPa of Young's modulus, and 3.14% elongation at maximum load. The chemical treatment and the fabricated composites reveal excellent mechanical properties due to better adhesion of fiber and matrix.

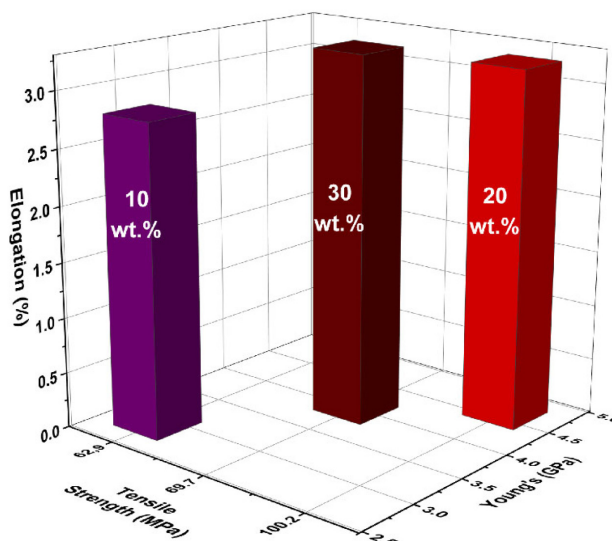


Figure 10. Mechanical properties of MEC samples

In other works,^{19,20,32} the best results found for the mechanical properties, tensile strength, Young's modulus, and elongation at maximum load obtained from Mallow fiber reinforced epoxy composites are those with 20 and 30 wt.%, as shown in Table 2.

Comparing the tensile strength obtained in this work with the other results presented in Table 2, we can observe that 100.22 MPa (20 wt.%) > 81.25 MPa (20 wt.)¹⁹ and 100.22 MPa (20 wt.%) > 56.2 MPa (30 wt.)²⁰ and 100.22 MPa (20 wt.%) > 69.75 MPa (30 wt.) and 100.22 MPa (20 wt.%) < 130.70 and 177.49 MPa

Table 2. Mechanical properties of Mallow/epoxy for the best fiber load

Fiber Loading (wt.%)	Tensile Strength (MPa)	Young's Modulus (GPa)	Elongation	Reference
20	81.25	3.98	22.2%	19
30	177.49	-	4.99 mm (silicone mold)	32
30	130.70	-	1.43 mm	32
30	56.2	15.8	-	20
20	100.22	4.59	3.14%	this work
30	69.75	4.00	3.29%	this work

(30 wt.%).³² This difference of 20% or 30% between the parameters of mechanical properties may be related to the mechanical characteristics of the natural fiber, which may be influenced by several factors such as processing techniques for fiber extraction, aspect ratio, cultivation conditions, matrix selection, interfacial strength, fiber distribution, stacking sequence, composite production process, and permeability since these are the primary elements that affect mechanical performance.⁶⁶

Figure 11 shows the SEM images of fractured cross-sections after a tensile test for MEC 10% (Figure 11a), 20% (Figure 11b), and 30% (Figure 11c) wt.%. Fracture analysis contributes to explaining the improvement provided by the Mallow fiber reinforcement to the epoxy matrix of the investigated composites. In Figures 11a and 11c, one can see the fiber/matrix interface after the tensile test and the matrix river marks this typical characteristic of fragile polymer fracture.⁶⁷ This is because the reinforcement

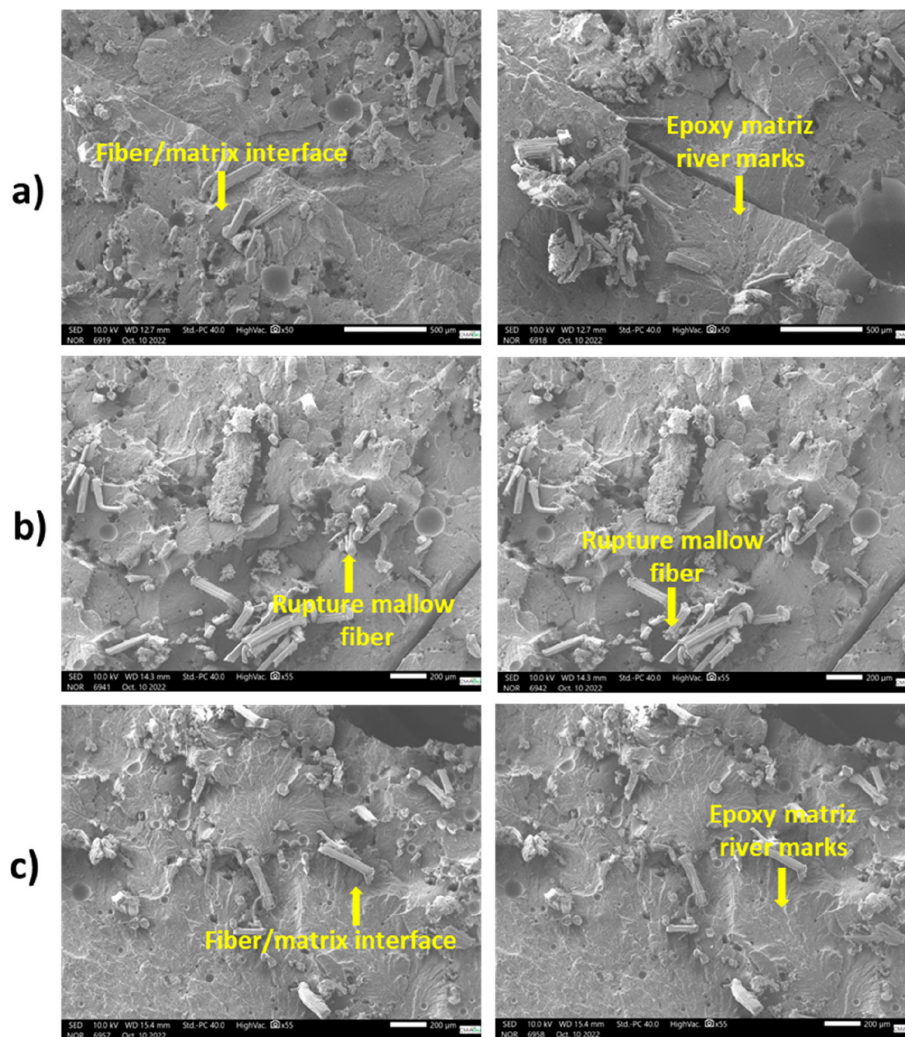


Figure 11. SEM images of fractured cross-sections from the MEC tensile test: (a) 10 wt.% (b) 20 wt.% (c) 30 wt.%

by the fibers is not yet effective, thus making the fracture mechanism fragile.^{20,32,50} A weak fiber/matrix interaction, in which load transfer from the matrix to the fiber is not effective, leads to a reduction in the tensile properties⁶⁸⁻⁷⁰ which also explains the tensile strength values obtained for the MEC with a fiber load of 10 wt.% and 30 wt.% being lower than that obtained for the MEC with 20 wt.%.

For the composites with 20% fiber loading present in Figure 11b, rupture fiber is observed. The main point to be observed in this figure is the well-adhered Mallow fiber into the epoxy matrix. The fiber rupture is more intense, as is the interfacial displacement with the epoxy matrix, evidenced by ruptured fibers, and only a few holes associated with fiber pullout were detected. The fiber failure mode indicates good load transfer through fibers and matrix improves the mechanical properties of natural fiber-reinforced polymer composites,²⁰ a fact corroborated by the higher mechanical resistance.

4. Conclusions

The Mallow fiber treated with 5% NaOH increased cellulose and lignin and removed hemicellulose and ash content. The effective removal of chemical groups, such as waxes, upon alkalization, was identified and confirmed via the Fourier Transform Infrared (FTIR) spectroscopy. The TMF presented higher crystallinity index (C_i) values than UTMF, thus indicating the effectiveness of the chemical treatment. Fibers such as Mallow, with a high crystallinity index, have low amorphous regions and result in stiff and strong fibers of interest in the formation of fiber composites. The UTMF has the highest amount of amorphous cellulose, which explains why the first exothermic peak temperature (DSC) is lower than those of the TMF, which has the least amount of amorphous cellulose. The scanning electron microscopy (SEM) results indicate that, after the alkali treatment, the Mallow fiber reveals an increase in surface roughness due to the chemical degradation, thus improving its physical adhesion with the matrix phase, and, consequently, increasing the mechanical properties of the composite material. In addition, the SEM analysis confirms an effective adhesion of the Mallow fiber to the epoxy matrix and the crack arrest by the fiber that contributes to the reinforcement behavior. Finally, treated Mallow fibers have high thermal stability and crystallinity index values, and 20 wt.% of fiber loading was considered to be the optimum fiber loading for the fabrication of Mallow/epoxy resin composites (MEC) as it shows the best mechanical properties (*i.e.*, 100.22 MPa of tensile strength, 4.59 GPa in Young's modulus) when compared with the other fabricated composites.

Acknowledgments

The authors would like to thank the Textile Company of the State of Pará, branch Manacapuru, AM, the CMABIO

and R&D laboratories of the Amazonas State University, the analytical center of the Federal Institute of Education of Amazonas, the physical-chemical testing laboratory of materials at the Federal University of Amazonas, and the Postgraduate Program in Chemistry of the Federal University of Amazonas for their support in this work, and to Coordenação de Aperfeiçoamento de Pessoal de Nível Superior - Brasil (CAPES) - Finance Code 001.

Author Contributions

Wamber Broni de Souza - research, original draft writing, writing-revision and editing; Genilson Pereira Santana - writing-revision and editing; Dorian L. de Oliveira - revision and editing; Antônio C. Kieling - revision and editing; José Costa de Macêdo Neto - revision and editing; Gilberto G. del Pino - revision and editing; Sérgio D. Júnior - revision and editing.

References

- Bartoli, M.; Giorcelli, M.; Tagliaferro, A.; Em *Handbook of Epoxy/Fiber Composites*; Mavinkere, R. S.; Parameswaranpillai, J.; Siengchin, S.; Thomas, S., eds.; Springer: Singapore, 2022. [Crossref]
- Natesan, K.; Kumaresan, K.; Sathish, S.; Gokulkumar, S.; Prabhu, L.; Vigneshkumar, N.; An overview: Natural fiber reinforced hybrid composites, chemical treatments and application areas. *Materials Today: Proceedings* **2020**, *27*, 2828. [Crossref]
- El-Wazery, M. S.; El-Elamy, M. I.; Zoalfakar, S. H.; Mechanical Properties of Glass Fiber Reinforced Polyester Composites. *International Journal of Applied Science and Engineering* **2017**, *14*, 121. [Crossref]
- Thomason, J. L.; Glass fibre sizing: A review. *Composites Part A: Applied Science and Manufacturing* **2019**, *127*, 105619. [Crossref]
- Koohestani, A. S.; Azadeh Bashari; Em *Advances in Functional and Protective Textiles*; Ul-Islam, S.; Butola, B. S., eds.; Woodhead: Philadelphia, 2020, Ch. 12.
- Tanzi, M. C.; Fare, S.; Candiani, G.; Organization, Structure, and Properties of Materials. Em *Foundations of Biomaterials Engineering*; Publisher: Elsevier, 2019, Ch. 1.
- Bhatt, P.; Goe, A.; Carbon Fibres: Production, Properties and Potential Use. *Material Science Research India* **2017**, *14*, 52. [Crossref]
- Park, S.-J.; Em *Carbon Fibers*; Springer: Berlin/Heidelberg: Singapore, 2018.
- Varley, D.; Yousaf, S.; Youseffi, M.; Mozafari, M.; Khurshid, Z.; Sefat, F.; Em *Advanced Dental Biomaterials*; Khurshid, Z.; Najeeb, S.; Zafar, M. S.; Sefat, F., eds.; Elsevier: Berlin/Heidelberg, 2019, Ch. 13.
- Bermudez, V. M.; Lukubira, S.; Ogale, A. A.; Em *Comprehensive Composite Materials II*; Elsevier:Oxford, 2018.

11. Ertekin, M.; Em *Fiber Technology for Fiber-Reinforced Composites*; Woodhead: Philadelphia, 2017.
12. Antov, P.; Savov, V.; Neykov, N.; Utilization of Agricultural Waste and Wood Industry Residues in the Production of Natural Fiber-Reinforced Composite Materials. *International Journal Wood Design and Technology* **2018**, *6*, 64. [[Crossref](#)]
13. Mohd Bakhori, S. N.; Hassan, M. Z.; Mohd Bakhori, N.; Jamaludin, K. R.; Ramlie, F.; Md Daud, M. Y.; Abdul Aziz, S.; Physical, Mechanical and Perforation Resistance of Natural-Synthetic Fiber Interply Laminate Hybrid Composites. *Polymers* **2022**, *14*, 1322. [[Crossref](#)].
14. Leão, A.; Sartor, S.; Caraschi, J.; Natural fibers-based composites - Technical and social issues. *Molecular Crystals and Liquid Crystals* **2006**, *448*, 161. [[Crossref](#)].
15. Savastano Jr, Holmer.; *Tese de Livre Docência*, Escola Politécnica – USP. 2000. [[Crossref](#)].
16. Noda, S. do N.; Em *A cultura de juta e malva na Amazônia Ocidental: sementes de uma nova racionalidade ambiental?*; Carlos, A.; Ferreira, A. da S.; Homma, A. K. O.; Fraxe, T. de J. P., eds.; Annablume: São Paulo, 2010.
17. Soares, F. I. L.; Silva, G. V.; Machado, V. M.; Oliveira, J. O. dos S.; Duarte, E. R.; Mota, F. dos S.; Sustentabilidade na agricultura familiar: um estudo na cadeia produtiva da juta (*Corchoruscapsularis*) em Alenquer/PA. *Brazilian Journal of Development* **2020**, *6*, 16652. [[Crossref](#)].
18. Fraxe, T. P. de J.; Ferreira, A. S.; Nova técnica para extração de fibras de juta e malva em processo a seco no Estado do Amazonas: o resgate da utopia. *Inclusão Social*. **2018**, *12*, 161.
19. Jena, P. K.; Mohanty, J. R.; Nayak, S.; Panda, K. R.; Sahu, R.; Khuntia, S. K.; Utilization of Chemically Modified Novel Urena Lobata Fibers as Reinforcement in Polymer Composites—an Experimental Study. *Journal of Natural Fibers* **2022**, *19*, 2479. [[Crossref](#)].
20. Margem, J. I.; Gomes, V. A.; Margem, F. M.; Ribeiro, C. G. D.; Braga, F. O.; Monteiro, S. N.; Flexural Behavior of Epoxy Matrix Composites Reinforced with Malva Fiber. *Materials Research-ibero-american Journal of Materials* **2015**, *18*, 114. [[Crossref](#)]
21. Moraes, Y. M.; Ribeiro, C. G. D.; Margem, F. M.; Monteiro, S. N.; Margem, J. I.; Em *Characterization of Minerals, Metals, and Materials*; Ikhmayes, S. J.; Li, B., orgs.; Downtow Nashville: Wiley, 2017.
22. Alagesan, P. K.; Em *Hybrid Fiber Composites*; Wiley: Hoboken: New Jersey, 2020.
23. Swolfs, Y.; Perspective for fibre-hybrid composites in wind energy applications. *Materials* **2017**, *10*, 1281. [[Crossref](#)]
24. Rajak, D. K.; Pagar, D. D.; Menezes, P. L.; Linul, E.; Fiber-reinforced polymer composites: Manufacturing, properties, and applications. *Polymers* **2019**, *11*, 2088. [[Crossref](#)].
25. Atmakuri, A.; Palevicius, A.; Vilkauskas, A.; Janusas, G.; Review of hybrid fiber based composites with nano particles-material properties and applications. *Polymers* **2020**, *12*, 2088. [[Crossref](#)].
26. Mat Kasim, F. A.; Roslan, S. A. H.; Rasid, Z. A.; Yakub, F.; Hassan, M. Z.; Yahaya, H.; Post-buckling of bamboo reinforced composite plates. *IOP Conference Series: Materials Science and Engineering* **2021**, *1051*, 012040. [[Crossref](#)]
27. Ravishankar, B.; Nayak, S. K.; Kader, M. A.; Hybrid composites for automotive applications – A review. *Journal of Reinforced Plastics and Composites* **2019**, *38*, 835. [[Crossref](#)]
28. Das, P. P.; Chaudhary, V.; Kumar Singh, R.; Singh, D.; Aditya Bachchan, A.; Em *Materials Today: Proceedings* Elsevier Ltd, 2021.
29. da Luz, F. S.; Junior, E. P. L.; Louro, L. H. L.; Ballistic test of multilayered armor with intermediate epoxy composite reinforced with jute fabric. *Materials Research* **2015**, *18*, 170. [[Crossref](#)]
30. Reis, R. H. M.; Nunes, L. F.; da Luz, F. S.; Candido, V. S.; da Silva, A. C. R.; Monteiro, S. N.M. Ballistic performance of guaruman fiber composites in multilayered armor system and as single target. *Polymers* **2021**, *13*, 1203. [[Crossref](#)]
31. da Luz, F. S.; Filho, F. C. G.; Oliveira, M. S.; Nascimento, L. F. C. N.; Monteiro, S. N.; Composites with natural fibers and conventional materials Applied in a hard armor: A comparison. *Polymers* **2020**, *12*, 1920. [[Crossref](#)]
32. Nascimento, L. F. C.; *Tese de Doutorado*, Instituto Militar de Engenharia, 2017. [[Link](#)]
33. del Pino, G. G.; Kieling, A. C.; Bezazi, A.; Boumediri, H.; Souza, J. F. R.; Díaz, F. R. V.; Rivera, J. L. V.; Dehaini, J.; Panzera, T. H.; Hybrid polyester composites reinforced with curauá fibres and nanoclays. *Fibers and Polymers* **2020**, *21*, 399. [[Crossref](#)]
34. Oliveira, L.; Santos, J. C.; Panzera, T. H.; Freire, R. T. S.; Vieira, L. M. G.; Scarpa, F.; Evaluation of hybrid-short-coir-fibre-reinforced composites via full factorial design. *Composite Structures* **2018**, *202*, 313. [[Crossref](#)]
35. Zuber, M.; Zia, K. M.; Bhatti, I. A.; Ali, Z.; Arshad, M. U.; Saif, M. J.; Modification of cellulosic fibers by UV-irradiation. Part II: After treatments effects. *International Journal of Biological Macromolecules* **2012**, *51*, 743. [[Crossref](#)] [[PubMed](#)]
36. Mohanty, A. K.; Misra, M.; Drzal, L. T.; Surface modifications of natural fibers and performance of the resulting biocomposites: An overview. *Composite Interfaces* **2001**, *8*, 313. [[Crossref](#)]
37. Van Soest, P. J.; Robertson, J. B.; Lewis, B. A.; Methods for Dietary Fiber, Neutral Detergent Fiber, and Nonstarch Polysaccharides in Relation to Animal Nutrition. *Journal of Dairy Science* **1991**, *74*, 3583. [[Crossref](#)] [[PubMed](#)]
38. ASTM D3418-03; *Standard Test Method for Transition Temperatures and Enthalpies of Fusion and Crystallization of Polymers by Differential Scanning Calorimetry* ASTM International: West Conshohocken, PA, 2003.
39. ASTM E2809-13; *Standard Guide for Using Scanning Electron Microscopy/X-ray Spectrometry in Forensic Paint Examinations* ASTM International: West Conshohocken, PA, 2013.
40. ASTM D638-14; *Standard Test Method for Tensile Properties of Plastics* ASTM International: West Conshohocken, PA, 2014.
41. Mwaikambo, L. Y.; Ansell, M. P.; Chemical modification of hemp, sisal, jute, and kapok fibers by alkalization. *Journal of Applied Polymer Science* **2002**, *84*, 2222. [[Crossref](#)]
42. Ferreira, F. C.; Curvelo, A. A. S.; Mattoso, L. H. C.; Preparation and characterization of benzylated sisal fibers. *Journal of Applied Polymer Science* **2003**, *89*, 2957. [[Crossref](#)]
43. Shanmugasundaram, N.; Rajendran, I.; Ramkumar, T.; Characterization of untreated and alkali treated new cellulosic

- fiber from an Areca palm leaf stalk as potential reinforcement in polymer composites. *Carbohydrate Polymers* **2018**, *195*, 566. [[Crossref](#)] [[PubMed](#)]
44. Lotfi, A.; Li, H.; Dao, D. V.; Prusty, G.; Natural fiber–reinforced composites: A review on material, manufacturing, and machinability. *Journal of Thermoplastic Composite Materials* **2021**, *34*, 238. [[Crossref](#)]
 45. Hassan, A.; Isa, M. R. M.; Ishak, Z. A. M.; Ishak, N. A.; Rahman, N. A.; Salleh, F. M.; Characterization of sodium hydroxide-treated kenaf fibres for biodegradable composite application. *High Performance Polymers* **2018**, *30*, 890. [[Crossref](#)]
 46. Sood, M.; Dwivedi, G.; Effect of fiber treatment on flexural properties of natural fiber reinforced composites: A review. *Egyptian Journal of Petroleum* **2018**, *27*, 775. [[Crossref](#)]
 47. Jones, D.; Ormondroyd, G. O.; Curling, S. F.; Popescu, C. M.; Popescu, M. C.; Em *Advanced High Strenght Natural Fibre Composites in Construction*; Elsevier: Amsterdam, 2017.
 48. Chokshi, S.; Parmar, V.; Gohil, P.; Chaudhary, V.; Chemical Composition and Mechanical Properties of Natural Fibers. *Journal of Natural Fibers* **2022**, *19*, 3942. [[Crossref](#)]
 49. Spinacé, M. A. S.; Lambert, C. S.; Fermoselli, K. K. G.; de Paoli, M. A.; Characterization of lignocellulosic curaua fibres. *Carbohydrate Polymers* **2009**, *77*, 47. [[Crossref](#)]
 50. del Pino, G. G.; Bezazi, A.; Boumediri, H.; Kieling, A. C.; Silva, C. C.; Dehaini, J.; Rivera, J. L. V.; Valenzuela, M. das G. da S.; Díaz, F. R. V.; Panzera, T. H.; Hybrid epoxy composites made from treated curauá fibres and organophilic clay. *Journal of Composite Materials* **2021**, *55*, 57. [[Crossref](#)]
 51. Sathishkumar, T. P.; Navaneethakrishnan, P.; Shankar, S.; Rajasekar, R.; Rajini, N.; Characterization of natural fiber and composites - A review. *Journal of Reinforced Plastics and Composites* **2013**, *32*, 1457. [[Crossref](#)]
 52. Satyanarayana, K. G.; Guimarães, J. L.; Wypych, F.; Studies on lignocellulosic fibers of Brazil. Part I: Source, production, morphology, properties and applications. *Composites Part A: Applied Science and Manufacturing* **2007**, *38*, 1694. [[Crossref](#)]
 53. Xu, F.; Yu, J.; Tesso, T.; Dowell, F.; Wang, D.; Qualitative and quantitative analysis of lignocellulosic biomass using infrared techniques: A mini-review. *Applied Energy* **2013**, *104*, 801. [[Crossref](#)]
 54. Nayak, S.; Mohanty, J. R.; Influence of chemical treatment on tensile strength, water absorption, surface morphology, and thermal analysis of areca sheath fibers. *Journal of Natural Fibers* **2019**, *16*, 589. [[Crossref](#)]
 55. González, M. G.; Valcárcel, J. C. C.; Llidó, J. B.; Applications of FTIR on Epoxy Resins - Identification, Monitoring the Curing Process, Phase Separation and Water Uptake. *Infrared Spectroscopy - Materials Science, Engineering and Technology*, Ed. T Theophanides. *IntechOpen* **2012**, 261 – Ch.13. [[Link](#)]
 56. Subramanian, K.; Kumar, P. S.; Jeyapal, P. Venkatesh, N.; Characterization of ligno-cellulosic seed fibre from wrightia tinctoria plant for textile applications – an exploratory investigation. *European Polymer Journal* **2005**, *41*, 853. [[Crossref](#)]
 57. d’Almeida, J. R. M.; Aquino, R. C. M. P.; Monteiro, S. N.; Tensile mechanical properties, morphological aspects and chemical characterization of piassava (*Attalea funifera*) fibres. *Composites Part A: Applied Science and Manufacturing* **2006**, *37*, 1473. [[Crossref](#)]
 58. Yang, H.; Yan, R.; Chen, H.; Lee, D. F.; Zheng, C.; Characteristics of hemicellulose, cellulose and lignin pyrolysis. *Fuel* **2007**, *86*, 1781. [[Crossref](#)]
 59. Tejado, A.; Pena, C.; Labidi, J.; Echeverria, J. M.; Mondragon, I.; Physicochemical characterization of lignins from different sources for use in phenolformaldehyde resin synthesis. *Bioresource Technology* **2007**, *98*, 1655. [[Crossref](#)]
 60. Garcia-Pérez, M.; Chaala, A.; Yang, J.; Roy, C.; Co-pyrolysis of sugarcane bagasse with petroleum residue. Part I: Thermogravimetric analysis. *Fuel* **2001**, *80*, 1245. [[Crossref](#)]
 61. Tserki, V.; Matzinos, P.; Kokkou, S.; Panayiotou, C.; Novel biodegradable composites based on treated lignocellulosic waste flour as filler. Part I. Surface chemical modification and characterization of waste flour. *Composites Part A: Applied Science and Manufacturing* **2005**, *36*, 965. [[Crossref](#)]
 62. Tserki, V.; Zafeiropoulos, N. E.; Simom, F.; Panayiotou, C.; A study of the effect of acetylation and propionylation surface treatments on natural fibres. *Composites Part A: Applied Science and Manufacturing* **2005**, *36*, 1110. [[Crossref](#)]
 63. Zafeiropoulos, N. E.; Williams, D. R.; Baillie, C. A.; Matthews, F. L.; Engineering and characterisation of the interface in flax fibre/polypropylene composite materials. Part I. Development and investigation of surface treatments. *Composites Part A: Applied Science and Manufacturing* **2022**, *33*, 1083. [[Crossref](#)]
 64. Rowell, R. M.; Sanadi, A. R.; Caul-Field, D. F.; Jacobson, R. E.; Rowell, R.; Sanadi, A.; Caulfield, D.; Jacobson, R.; *Utilization of Natural Fibers in Plastic Composites: Problems and Opportunities Lignocellulosic-Plastics Composites*. Em *Lignocellulosic-plastics Composites*; 1997.
 65. Chand, N.; Hashmi, S. A. R.; Mechanical properties of sisal fibre at elevated temperatures. *Journal of Materials Science* **1993**, *28*, 6724. [[Crossref](#)]
 66. Jariwala, H.; Jain, P.; A review on mechanical behavior of natural fiber reinforced polymer composites and its applications. *Journal of Reinforced Plastics and Composites* **2019**, *38*, 441. [[Crossref](#)]
 67. Oliveira, M. S.; da Luz, F. S.; Souza, A. T.; Demosthenes, L. C. C.; Pereira, A. C.; Filho, F. C. G.; Braga, F. O.; Figueiredo, A. B. S.; Monteiro, S. N.; Tucum fiber amazon *astrocaryum vulgare* palm tree: Novel reinforcement for Polymer composites. *Polymers* **2020**, *12*, 2259. [[Crossref](#)]
 68. Sydenstricker, T. H. D.; Mochnaz, S.; Amico, S. C.; Pull-out and other evaluations in sisal-reinforced polyester biocomposites. *Polymer Testing* **2003**, *22*, 375. [[Crossref](#)]
 69. Viel, Q.; Esposito, A.; Saiter, J. M.; Santulli, C. Turner, J. A.; Interfacial characterization by pull-out test of bamboo fibers embedded in poly (lactic acid). *Fibers* **2018**, *6*, 7. [[Crossref](#)]
 70. Hsueh, C. H.; Interfacial debonding and fiber pull-out stresses of fiber-reinforced composites III: With residual radial and axial stresses. *Materials Science and Engineering* **1991**, *145*, 135. [[Crossref](#)]